Phosphorylation by cAMP-Dependent Protein Kinase Modulates the Structural Coupling between the Transmembrane and Cytosolic Domains of Phospholamban[†]

Jinhui Li and Diana J. Bigelow

School of Molecular Biosciences, Washington State University Tri-Cities, Richland, Washington 99352

Thomas C. Squier*

Cell Biology Group, Biological Sciences Department, Pacific Northwest National Laboratory, Richland, Washington 99352

Received May 2, 2003; Revised Manuscript Received July 16, 2003

ABSTRACT: We have used frequency-domain fluorescence spectroscopy to investigate the structural linkage between the transmembrane and cytosolic domains of the regulatory protein phospholamban (PLB). Using an engineered PLB having a single cysteine (Cys^{24}) derivatized with the fluorophore *N*-(1-pyrenyl)maleimide (PMal), we have used fluorescence resonance energy transfer (FRET) to measure the average spatial separation and conformational heterogeneity between PMal bound to Cys^{24} in the transmembrane domain and Tyr^{6} in the cytosolic domain near the amino terminus of PLB. In these measurements, PMal serves as a FRET donor, and Tyr^{6} serves as a FRET acceptor following its nitration by tetranitromethane. The native structure of PLB is retained following site-directed mutagenesis and chemical modification, as indicated by the ability of the derivatized PLB to fully regulate the Ca-ATPase following their co-reconstitution. To assess how phosphorylation modulates the structure of PLB itself, FRET measurements were made following reconstitution of PLB in membrane vesicles made from extracted sarcoplasmic reticulum membrane lipids. We find that the cytosolic domain of PLB assumes a wide range of conformations relative to the transmembrane sequence, consistent with other structural data indicating the presence of a flexible hinge region between the transmembrane and cytosolic domains of PLB. Phosphorylation of Ser^{16} by PKA results in a 3 Å decrease in the spatial separation between PMal at Cys^{24} and nitroTyr^{6} and an almost 2-fold decrease in conformational heterogeneity, suggesting a stabilization of the hinge region of PLB possibly through an electrostatic linkage between phosphoSer^{16} and Arg^{13} that promotes a coil-to-helix transition. This structural transition has the potential to function as a conformational switch, since inhibition of the Ca-ATPase requires disruption of the secondary structure of PLB in the vicinity of the hinge element to permit association with the nucleotide binding domain at a site located approximately 50 Å above the membrane surface. Following phosphorylation, the stabilization of the helical content in the hinge domain will disrupt this inhibitory interaction by reducing the maximal dimension of the cytosolic domain of PLB. Thus, stabilization of the structure of PLB following phosphorylation of Ser^{16} is part of a switching mechanism, which functions to alter binding interactions between PLB and the nucleotide binding domain of the Ca-ATPase that modulates enzyme inhibition.

Phospholamban (PLB)[1] represents a major target of the β-adrenergic cascade, and its phosphorylation at Ser^{16} by cAMP-dependent protein kinase (PKA) results in the release of the inhibitory interaction between PLB and the Ca-ATPase, resulting in accelerated rates of muscle relaxation that facilitates greater cardiac force generation (*1*−*8*). PLB binding to the Ca-ATPase inhibits transport activity by restricting catalytically important motions involving the nucleotide binding domain of the Ca-ATPase known to be involved in calcium transport (*9*−*14*). Release of inhibition is mediated by the phosphorylation of PLB by PKA, which induces a structural change near the putative hinge of PLB that relaxes the conformational restriction of the nucleotide binding domain (*11*, *15*). However, the nature of the conformational switch involving the phosphorylation-dependent change in the structure of PLB that underlies regulation of the Ca-ATPase remains undefined.

Knowledge of the binding site for PLB on the Ca-ATPase coupled with recent high-resolution structures of PLB and the Ca-ATPase provides important insights into the interaction between PLB and the Ca-ATPase and suggests that the inhibitory interaction between PLB and the Ca-ATPase requires PLB to adopt an extended structure (*12*, *13*, *16*−*19*). From the high-resolution NMR structure, PLB is

[†] This work was supported by a grant from the National Institutes of Health (HL64031).

* Correspondence should be addressed to this author at Pacific Northwest National Laboratory, P.O. Box 999, Mail Stop P7-53, Richland, WA 99352. E-mail: thomas.squier@pnl.gov.

[1] Abbreviations: ATP, adenosine 5′-triphosphate; cAMP, adenosine 3′,5′-cyclic monophosphate; CCCP, carbonyl cyanide 3-chlorophenylhydrazone; $C_{12}E_9$, polyoxyethylene 9 lauryl ether; EGTA, ethylene glycol bis(β-aminoethyl ether)-*N*,*N*,*N*′,*N*′-tetraacetic acid; OG, *n*-octyl β-D-glucopyranoside; PKA, cAMP-dependent protein kinase; PLB, phospholamban; PMal, *N*-(1-pyrenyl)maleimide; POPOP, 1,4-bis(5-phenyl-2-oxazolyl)benzene; SDS, sodium dodecyl sulfate; SDS−PAGE, sodium dodecyl sulfate−polyacrylamide gel electrophoresis; SERCA, sarco(endo)plasmic Ca-ATPase; SR, sarcoplasmic reticulum.

10.1021/bi034708c CCC: $25.00
Published on Web 08/20/2003

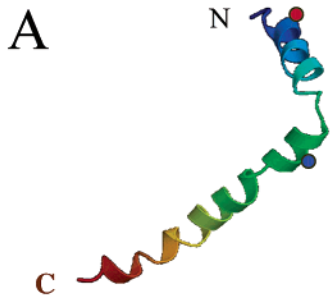

FIGURE 1: Depiction of backbone fold (A) and primary sequence (B) of PLB showing relative positions of donor chromophore PMal (blue circle) covalently bound to position 24 and acceptor chromophore nitrotyrosine (red circle) at position 6 relative to the complete amino acid sequence. The illustration was taken from the Protein Data Bank using the coordinates published by Krebs and co-workers (1FJK.pdb; *16*).

suggested to form transmembrane (residues 22−49) and cytosolic (residues 4−16) helical domains connected through either a β- or flexible-turn conformation (Figure 1), permitting the cytosolic domain of PLB to adopt a range of conformations relative to the transmembrane domain (*16*, *20*, *21*).

These suggestions are consistent with some earlier FTIR measurements of PLB in reconstituted bilayers, which also suggested that PLB is composed of two α-helices separated by a β-structure (*22*). However, an alternative model based on similar FTIR measurements of PLB reconstituted into lipid bilayers suggests that PLB adopts a continuous α-helix of about 40 amino acids (*23*, *24*). Moreover, spin-label EPR and solid-state NMR measurements of PLB in reconstituted bilayers have been interpreted to indicate that the cytosolic domain of PLB orients approximately perpendicular to the plane of the membrane so as to undergo direct binding interactions with the lipid bilayer (*25*, *26*). These contradictory models suggest two possibilities: one, that the high-resolution structures of PLB obtained in organic cosolvents or helix-promoting solvents at low pH do not reflect the native structure of PLB in the bilayer; the other, that the spin-label electron paramagnetic resonance (EPR) and solid-state nuclear magnetic resonance (NMR) measurements, which resolve a single average structural intermediate, do not resolve the biological conformational heterogeneity.

To further investigate the structure of PLB and phosphorylation-induced structural changes, we have used fluorescence resonance energy transfer (FRET) to measure the spatial separation and conformational heterogeneity between chromophores located in the cytosolic and transmembrane domains of PLB following reconstitution into membrane bilayers made from lipids extracted from sarcoplasmic reticulum (SR) membranes. These measurements demonstrate the presence of considerable conformational heterogeneity with respect to the relative orientations of the cytosolic and transmembrane domains that is reduced following the phosphorylation of Ser[16] in PLB by PKA. The phosphorylation-induced restriction in conformational heterogeneity indicates the stabilization of the backbone fold of PLB, suggesting that the linker between the cytosolic and transmembrane domains becomes more ordered due to a coil-to-helix structural transition.

EXPERIMENTAL PROCEDURES

Materials. *N*-(1-Pyrenyl)maleimide (PMal) was obtained from Molecular Probes, Inc. (Junction City, OR). Tetranitromethane (TNM) was purchased from Aldrich (Milwaukee, WI). Polyoxyethylene 9 lauryl ether ($C_{12}E_9$), cAMP-dependent protein kinase (PKA), cAMP, ATP, $MgCl_2$, the calcium ionophore A23187, EGTA, DEAE-cellulose, and *n*-octyl β-D-glucopyranoside (OG) were purchased from Sigma (St. Louis, MO). 3-(*N*-morpholino)propanesulfonic acid (MOPS) was purchased from Fisher Biotech (Fair Lawn, NJ). Bio-Beads SM2 and acrylamide were purchased from Bio-Rad (Richmond, CA). Lipids were extracted from the SR vesicles isolated from rabbit skeletal fast-twitch muscle by standard methods (*27*, *28*). The Ca-ATPase was affinity purified from skeletal muscle SR using Reactive Red−agarose (*29*). Affinity-purified PLB and Ca-ATPase were stored at −70 °C.

Expression and Purification of PLB. DNA encoding the single cysteine mutant PLB (PLB, Cys[36,41,46]/Ala[24]Cys) was cloned into a pGEX-2T plasmid expression vector and expressed in JM109 *Escherichia coli* cells as previously described (*30*). The expressed PLB protein was purified by preparative electrophoresis essentially as previously described, with the exception that the *E. coli* cells were incubated with 200 μg/mL lysozyme at room temperature prior to sonication. The resulting membrane pellet collected by centrifugation at 150000*g* for 10 min was solubilized with 1% sarcosyl in 20 mM Tris-HCl (pH 7.5).

Co-reconstitution of the Ca-ATPase with PLB. Before reconstitution, the anionic detergent SDS in the purified PLB sample obtained from preparative SDS−PAGE was exchanged for nonionic detergent $C_{12}E_9$ using a DEAE-cellulose chromatography. This step involved application of approximately 2 mg of purified PLB in 10 mL of buffer containing 20 mM MOPS (pH 7.0) and 2.5% $C_{12}E_9$ onto the DEAE-cellulose column preequilibrated with the same buffer. PLB was eluted with 20 mM MOPS (pH 7.0), 2.5% $C_{12}E_9$, and 0.2 M NaCl. PLB was reconstituted in the absence or presence of purified Ca-ATPase at a molar ratio of three PLB per Ca-ATPase into liposomes of extracted SR lipids as previously described (*31*). The concentration of PLB was determined by the Amido Black method (*32*).

Enzyme, Protein, and Free Calcium Assays. ATP hydrolysis activity of the Ca-ATPase was determined by measuring the time course of the release of inorganic phosphate (*33*), using 100 g of protein/mL in a solution containing 50 mM MOPS (pH 7.0), 0.1 M KCl, 5 mM $MgCl_2$, 1 mM EGTA, 1 μM CCCP, 2 μM valinomycin, 2 μM A23187, and sufficient calcium to yield the desired concentration of free calcium (*31*). To phosphorylate PLB for enzyme activity measurements, 10 μg of PKA/mL and 1 μM cAMP were also included in the assay buffer, incubating the solution at 25

°C for 10 min before addition of 5 mM ATP to start the reaction. All protein concentrations were determined by the Amido Black method (*32*). Free calcium concentrations were calculated from total ligand and EGTA concentrations, correcting for pH and ionic conditions (*34*).

Specific Derivatization of PLB. The chemical modification of the single Cys^{24} with PMal and the nitration of the single Tyr^6 with tetranitromethane (TNM) was carried out essentially as previously described for other proteins (*35*, *36*). Before modification of Cys^{24} with PMal, PLB was incubated in the presence of 50 mM K_2HPO_4 (pH 7.2), 50 mM DTT, and 0.1% $C_{12}E_9$ for 3 h at room temperature. Following the separation of PLB from DTT using a Sephadex G-15 size-exclusion column, 6 μM PLB was incubated with 12 μM PMal in buffer A [50 mM K_2PO_4 (pH 7.2) and 0.1% $C_{12}E_9$] at 25 °C for 3 h. The reaction was quenched by the addition of 0.1 mM DTT before separating the labeled PLB from PMal using DEAE anion-exchange chromatography. After extensive washing, the bound PLB was eluted with buffer A containing 0.5 M NaCl. Incorporation of PMal was determined in buffer A using the molar extinction coefficient $\epsilon_{343nm} = 3.6 \times 10^4\ M^{-1}\ cm^{-1}$ (*37*). For nitration of Tyr^6, 6 μM PLB was suspended in 0.1 M Tris-HCl (pH 8.0), 1 M NaCl, and 0.1% $C_{12}E_9$ before the addition of 24 μM TNM, which was incubated at 25 °C for 1 h. PLB was then separated into 10 mM Tris-HCl buffer (pH 8.0) using a Sephadex G-15 size-exclusion column. The extent of nitration was determined following solubilization in 10 mM Tris-HCl (pH 8.0), 0.5 M NaCl, and 0.1% $C_{12}E_9$ using the molar extinction coefficient $\epsilon_{428nm} = 4200\ M^{-1}\ cm^{-1}$ (*38*).

Fluorescence Measurements. Steady-state fluorescence spectra were measured using a Spex Industries (Edison, NJ) Fluoromax-2 spectrofluorometer. Frequency-domain data (lifetime and anisotropy) were measured using an ISS K2 frequency-domain fluorometer (ISS Inc., Champaign, IL), as described previously (*39*). Excitation used the 333 nm output from a Coherent (Santa Clara, CA) Innova 400 argon ion laser; emitted light was collected after a Corion 400 nm interference filter (HW = 10 nm) using 1,4-bis(5-phenyl-2-oxazolyl)benzene (POPOP) in methanol (lifetime of 1.35 ns) as a lifetime reference. Measurements were made at 25 °C.

Analysis of Frequency-Domain Data. Explicit expressions, previously described in detail, permit the ready calculation of the lifetime components (i.e., α_i and τ_i) relating to a multiexponential decay or the Gaussian distribution of distances between donor and acceptor chromophores (*39*−*44*). In the case of FRET measurements, the incomplete nitration of Tyr^6 was taken into account, as previously described (*45*). Alternatively, algorithms are available that permit the determination of the initial anisotropy in the absence of rotational diffusion (r_0), the rotational correlation times (φ_i), and the amplitudes of the total anisotropy loss associated with each rotational correlation time ($r_0 g_i$), as previously described in detail (*36*). The parameter values are determined using the method of nonlinear least-squares analysis in which the reduced chi-squared (i.e., χ^2_R) are minimized (*46*). A comparison of χ^2_R values provides a quantitative assessment of the adequacy of different assumed models to describe the data (*47*). Data were fit using the Globals software package (University of Illinois, Urbana−Champaign) or the program Mathcad (MathSoft Inc., Cambridge, MA).

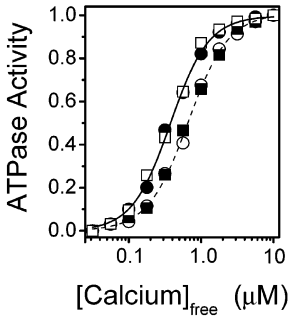

FIGURE 2: Calcium dependence of ATPase activity for the Ca-ATPase reconstituted with PLB in the absence (○, ■) or presence (●, □) of PKA for wild-type PLB (○, ●) or following covalent attachment of PMal to Cys^{24} and nitration of Tyr^6 (■, □). Calcium concentrations associated with half-maximal activation of the Ca-ATPase were 650 ± 20 nM (○), 660 ± 20 nM (■), 370 ± 10 nM (●), and 380 ± 10 nM (□). The maximal Ca^{2+}-dependent ATPase activities measured at 25 °C were 7.2 ± 0.2 (○), 7.5 ± 0.2 (●), 7.0 ± 0.1 (■), and 7.1 ± 0.2 (□) μmol of $P_i \cdot mg^{-1} \cdot min^{-1}$.

RESULTS

Function of Engineered and Derivatized PLB. A single cysteine mutant of PLB (A24C) was constructed in which the three cysteines in the transmembrane sequence (Cys^{36}, Cys^{41}, and Cys^{46}) of wild-type PLB were substituted with alanines, and a further substitution was introduced into the transmembrane sequence near the lipid−water interface to permit site-specific incorporation of the fluorescent probe *N*-(1-pyrenyl)maleimide (PMal) (Figure 1). Following derivatization with PMal, the A24C mutant of PLB migrates as a single monomeric species on SDS−PAGE (data not shown). This result is consistent with earlier measurements where it was demonstrated that following mutation of the three transmembrane cysteines to alanines oligomeric interactions are disrupted and PLB exists predominantly as a monomer (*48*−*50*). Thus, using this mutant of PLB there are no complications in the analysis of FRET between proximal PLB molecules within oligomeric species (*51*). While our structural measurements consider only PLB reconstituted into membrane lipids in the absence of the Ca-ATPase, we have additionally examined the ability of mutant and derivatized PLB to regulate the Ca-ATPase to investigate the possible effect of chemical derivatization on the structure of PLB. In agreement with earlier observations (*15*), the expressed PLB fully regulates the Ca-ATPase following co-reconstitution into liposomes made from SR lipids (Figure 2). This inhibitory interaction is evidenced by the characteristic shift in calcium concentration dependence of activation toward higher calcium in the presence of PLB and its reversal by PKA-dependent phosphorylation of PLB. Moreover, there is quantitative agreement between both the calcium concentrations required for half-maximal enzyme activation of the Ca-ATPase ($Ca_{1/2}$) in the absence and presence of PKA and the extent of the phosphorylation-induced shift in $Ca_{1/2}$ (i.e., $\Delta Ca_{1/2} = 280 \pm 20$ nM; Figure 2) and these values observed for the Ca-ATPase in cardiac microsomes ($\Delta Ca_{1/2} = 280 \pm 20$ nM; *52*, *53*). These results support earlier conclusions that the inhibitory form of PLB that associates with the Ca-ATPase is monomeric (*53*, *54*).

Table 1: Spatial Separation between PMal Bound to Cys^{24} and Tyr^{6} [a]

exptl conditions	E[b] (%)	R_0[c] (Å)	r_{app}[d] (Å)	R_{av}[e] (Å)	HW[e] (Å)	χ^2_R[f]
no PKA	31 ± 7	18.5 ± 0.1	21.1 ± 0.9	<21	36.3 (18.9−42.8)	12.0
+PKA	46 ± 5	17.7 ± 0.1	18.2 ± 0.6	12.3 (9.0−14.7)	15.0 (11.9−17.7)	8.9

[a] Values and associated errors were obtained from five to ten independent measurements of FRET between PMal−Cys^{24} and nitroTyr^{6} using 1 μM PLB in 50 mM MOPS (pH 7.0), 0.1 M KCl, 5 mM $MgCl_2$, 1 mM EGTA, and 0.55 mM $CaCl_2$, resulting in the presence of 0.5 μM free calcium in the absence and presence of PKA, where the fractional nitration of Tyr^{6} was 0.92. [b] Energy transfer efficiencies (E) represent average values and associated standard errors of the mean calculated using lifetime measurements of PMal−Cys^{24} in Table 2. [c] Förster critical distance (R_0) under the indicated experimental conditions represents the distance between chromophores where the FRET efficiency is 50% (*66*, *67*). [d] Apparent distance between PMal−Cys^{24} and nitroTyr^{6} calculated on the assumption of a unique conformation. [e] Average donor−acceptor distance (R_{av}) or full width at half-maximum (HW) assuming a Gaussian distribution of distances (*40*, *43*, *44*). Indicated errors were obtained from a global analysis of errors, as depicted in Figure 6. [f] Average value of the reduced chi-squared (χ^2_R) fit to the Gaussian distribution of distances.

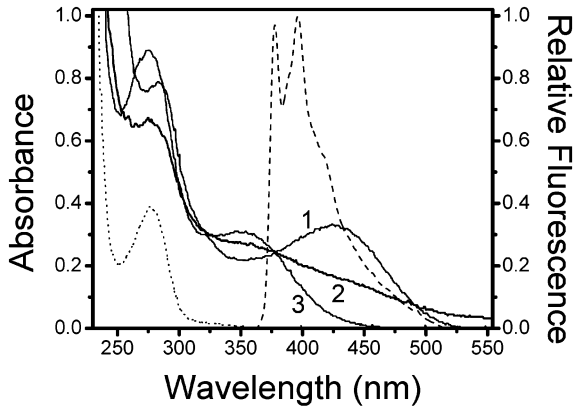

FIGURE 3: Spectral overlap between the steady-state emission spectrum of *N*-(1-pyrenyl)maleimide-labeled PLB (dashed line; λ_{ex} = 343 nm) and absorbance spectra of nitroTyr^{6} in PLB (solid line 2) for 41.5 μM PLB in 10 mM Tris-HCl (pH 7.0), 0.5 M NaCl, and 0.1% $C_{12}E_9$ (25 °C). Additional absorbance spectra of nitrated PLB are shown at pH 8.0 (solid line 1) and pH 3.5 (solid line 3), illustrating the sensitivity of the absorbance of nitrotyrosine to protonation. The absorbance spectrum of unlabeled PLB (dotted line) is shown for comparison.

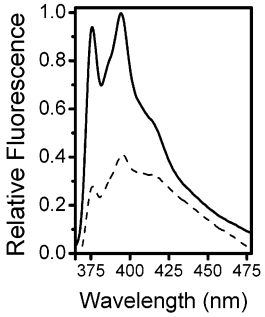

FIGURE 4: Steady-state emission spectra of PMal bound to Cys^{24} before (—) and following (---) nitration of Tyr^{6} for 4 μM PLB in 50 mM MOPS (pH 7.0), 0.1 M KCl, 5 mM $MgCl_2$, 1 mM EGTA, and 0.55 mM $CaCl_2$, resulting in 0.5 mM free calcium (25 °C). λ_{ex} = 343 nm.

Following covalent modification of Cys^{24} with PMal and nitration of Tyr^{6}, PLB retains its ability to fully inhibit the Ca-ATPase, which is fully reversed by phosphorylation by PKA (Figure 2). Thus, measurements of the spatial separation between PMal and nitroTyr^{6} reflect the physiological structure of PLB, and these samples will provide reliable information regarding the conformational switching mechanism underlying the regulation of the structure of PLB by PKA.

Spatial Separation between Sites on Transmembrane and Cytosolic Domains of PLB. The spectral overlap between the fluorescence emission spectrum of PMal covalently bound to Cys^{24} and the absorbance spectrum of nitroTyr^{6} permits the use of FRET to measure the spatial separation between these sites (Figure 3). Following nitration of Tyr^{6} the intensity of the fluorescence emission spectrum of PMal decreases by approximately 50% (Figure 4). These results suggest that the average spatial separation between PMal bound to Cys^{24} and nitroTyr^{6} is about 20 Å (i.e., approximately R_0; Table 1), consistent with previous NMR measurements of PLB in organic solvents. The average spatial separation between the side chains at positions 24 and 6 in the proposed average NMR structure varies between 19.1 and 25.2 Å (1FJK.pdb; *16*). Moreover, previous FTIR measurements also suggested that PLB is composed of two α-helices separated by a β-structure (*22*). However, these FRET measurements are inconsistent with an alternative model in which PLB forms a continuous α-helix where the average spatial separation between PMal covalently bound to Cys^{24} and nitroTyr^{6} would be approximately 28.5 Å (*23*, *24*).

Fluorescence Lifetime Measurements. Frequency-domain fluorescence spectroscopy was used to measure of the intensity decay of PMal bound to Cys^{24} in PLB in the absence and presence of nitroTyr^{6} (Figure 5), permitting an assessment of protein conformational heterogeneity. In the presence of nitrotyrosine the frequency response of PMal is shifted to the right, indicating that the average lifetime is reduced because of the presence of FRET. In both cases, the fluorescence intensity decay can be described as a sum of four exponentials, as indicated by the weighted residuals that are randomly distributed about the origin. The mean lifetime decreases from 3.2 ± 0.2 ns for PMal alone to 2.2 ± 0.2 ns in the presence of the FRET acceptor nitroTyr^{6} (Table 2). Assuming a single unique conformation of PLB, the decrease in average lifetime can be used to calculate an apparent spatial separation, which is 21.1 ± 0.9 Å (Table 1). These results are consistent with the steady-state fluorescence measurements and thus indicate that there is minimal static quenching which would indicate a significant population of PLB conformations that bring nitroTyr^{6} within 9 Å (i.e., $^1/_2R_0$) of PMal bound to Cys^{24}. Therefore, from this distance it is apparent that PLB adopts an extended structure upon reconstitution in liposomes.

Phosphorylation-Induced Structural Changes in PLB. Following phosphorylation of Ser^{16} by PKA there is a significant shift in the frequency response of PMal-labeled PLB toward lower frequencies (Figure 5B), indicating that the average lifetime increases. These results indicate that

Table 2: Lifetime Data for PMal Covalently Bound to Cys[24] in the Absence and Presence of the FRET Acceptor NitroTyr[99] [a]

exptl conditions[b]	label	α_1	τ_1 (ns)	α_2	τ_2 (ns)	α_3	τ_3 (ns)	α_4	τ_4 (ns)	$\bar{\tau}$ (ns)	χ^2_R [c]
no PKA	donor	0.61 ± 0.06	0.5 ± 0.1	0.27 ± 0.02	2.9 ± 0.8	0.10 ± 0.04	10 ± 2	0.02 ± 0.01	55 ± 2	3.2 ± 0.2	6.3
	D−A	0.69 ± 0.02	0.3 ± 0.1	0.22 ± 0.01	2.6 ± 0.5	0.08 ± 0.02	10 ± 2	0.01 ± 0.01	64 ± 5	2.2 ± 0.2	1.6
+PKA	donor	0.54 ± 0.05	0.5 ± 0.2	0.28 ± 0.03	3.1 ± 0.8	0.13 ± 0.03	11 ± 2	0.05 ± 0.02	70 ± 10	6.1 ± 0.5	5.1
	D−A	0.64 ± 0.02	0.4 ± 0.1	0.24 ± 0.01	2.7 ± 0.2	0.10 ± 0.02	10 ± 1	0.02 ± 0.01	70 ± 10	3.3 ± 0.1	6.5

[a] Indicated values and associated standard errors of the mean for three to six independent measurements were obtained from a four-exponential fit to frequency-domain data collected for PMal covalently bound to Cys[24] prior to (donor) or following (D−A) nitration of Tyr[6]. [b] Buffer contained 50 mM MOPS (pH 7.0), 0.1 M KCl, 5 mM $MgCl_2$, 5 mM ATP, 1 mM EGTA, and 0.6 mM $CaCl_2$ (free calcium concentration equals 0.5 μM) in the absence (no PKA) and presence (+PKA) of 1.0 μM cAMP and 20 μg PKA. The total volume was 2 mL. [c] Average value of the reduced chi-squared (χ^2_R) fit to the Gaussian distribution of distances.

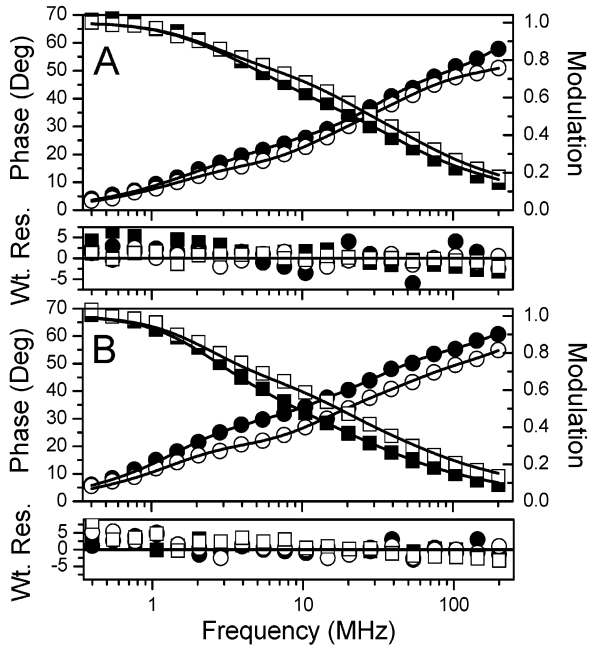

FIGURE 5: Frequency-domain lifetime data for PMal bound to PLB. Frequency response and four-exponential fit (black line, gray line) corresponding to the phase shift (●, ○) and modulation (■, □) for PMal−PLB in the absence (●, ■) and presence (○, □) of the FRET acceptor nitroTyr[6] for PLB in the absence (A) and presence (B) of PKA. Measurements were made at 25 °C using 0.2 μg/mL PLB in 50 mM MOPS (pH 7.0), 0.1 M KCl, 5 mM $MgCl_2$, 1 mM EGTA, and 0.55 mM $CaCl_2$, resulting in a free calcium concentration of 0.5 μM. Data were fit to a sum of exponentials, where $I(t) = \sum_i \alpha_i e^{-t/\tau_i}$ and the mean lifetime ($\bar{\tau}$) was calculated as $\sum_i \alpha_i \tau_i$. Lower panels below respective data sets represent the weighted residuals (i.e., the difference between the experimental data and the calculated fit divided by the experimental uncertainty) for models involving four-exponential fit to the data.

phosphorylation of PLB by PKA induces a substantial change in the structure of PLB in the vicinity of PMal covalently bound to Cys[24]. Moreover, in comparison to unphosphorylated PLB, the presence of nitroTyr[6] results in a larger shift in the frequency response toward higher frequencies, indicating that there is greater energy transfer efficiency. These results indicate that the average spatial separation between PMal bound to Cys[24] and nitroTyr[6] is reduced following phosphorylation by PKA. Using the mean lifetimes (i.e., $\bar{\tau}$) calculated from the multiexponential fits to the frequency-domain data (Table 2), the energy transfer efficiency increases from 31 ± 7% to 46 ± 5% following the phosphorylation of PLB by PKA. Assuming a unique donor−acceptor separation, these results suggest that the average spatial separation between PMal covalently bound to Cys[24] and nitroTyr[6] decreases from 21.1 ± 0.9 Å to 18.2 ± 0.6 Å following the phosphorylation of PLB. Thus phosphorylation of Ser[16] induces a conformational rearrangement that brings the transmembrane and cytosolic domains of PLB into closer proximity.

Conformational Heterogeneity of the Cytosolic Domain of PLB. Additional information regarding the average spatial separation and conformational heterogeneity between PMal and nitroTyr[6] located respectively on the transmembrane and cytosolic domains of PLB is available from fitting the time-dependent decays of PMal to a model that assumes a Gaussian distribution of distances between donor and acceptor chromophores (*40*, *43*, *55*). The intensity decay of PMal covalently bound to Cys[24] can be adequately described as a sum of four exponentials, as indicated by the random distribution of the weighted residuals about the origin (Figure 5). Inclusion of additional fitting parameters results in no further improvement of χ^2_R. The similar goodness of fit (i.e., χ^2_R) obtained when fitting the lifetime data to a model that assumes a Gaussian distribution of distances with two floating parameters (i.e., R_{av} and HW; Table 1) in comparison to the fit obtained using a sum of exponentials with nine floating parameters (i.e., α_1, τ_1, α_2, τ_2, α_3, τ_3, and τ_4; Table 2) indicates that fitting the data to the simpler model involving a distribution of distances is statistically justified.

From the distance distribution data it is apparent that the apparent spatial separation (r_{app}) calculated on the assumption of a unique donor−acceptor separation is consistent with the average spatial separation (R_{av}) determined from the distance distribution model (Table 1). The observed HW (full width at half-maximum height) of the donor−acceptor distance distribution of PLB in reconstituted bilayers is about 36 Å, indicating that the cytoplasmic domain of PLB adopts a wide distribution of conformations. The large extent of conformational heterogeneity is consistent with the presence of a flexible hinge connecting cytoplasmic and transmembrane domains of PLB and permitting a wide distribution of conformations within the cytoplasmic domain of PLB when the transmembrane domain is tethered within the bilayer. These results are inconsistent with models that assume PLB to be a continuous helix or that propose that the cytoplasmic domain directly binds to phospholipids at the membrane surface (*23*−*25*).

Following the phosphorylation of Ser[16] by PKA there is significant reduction in the half-width (HW) of the distribution, with no significant change in average spatial separation (R_{av}) (Table 1). A consideration of the error surfaces for these calculated distance distributions provides a conservative estimate of the recovered parameters (*56*) and demonstrates

Table 3: Rotational Dynamics of PMal Bound to Cys[24] in PLB[a]

exptl conditions[b]	r_0	$g_1 \times r_0$	φ_1 (ns)	$g_2 \times r_0$	φ_2 (ns)	φ_3 (ns)	χ^2_R[c]
no PKA	0.34 ± 0.02	0.15 ± 0.01	0.4 ± 0.2	0.11 ± 0.01	9 ± 3	200 ± 100	8.9
+PKA	0.33 ± 0.07	0.15 ± 0.05	0.2 ± 0.1	0.12 ± 0.04	7 ± 3	400 ± 200	12.0

[a] Mean values and associated standard errors of the mean obtained from a four-exponential fit to frequency-domain data collected for PMal bound to Cys[24], as described in the legend to Figure 5. [b] Associated errors obtained from error surfaces associated with simultaneous fits to three independent measurements obtained from a global fit to three data sets (*56*). [c] Average value of the reduced chi-squared (χ^2_R) fit to the Gaussian distribution of distances.

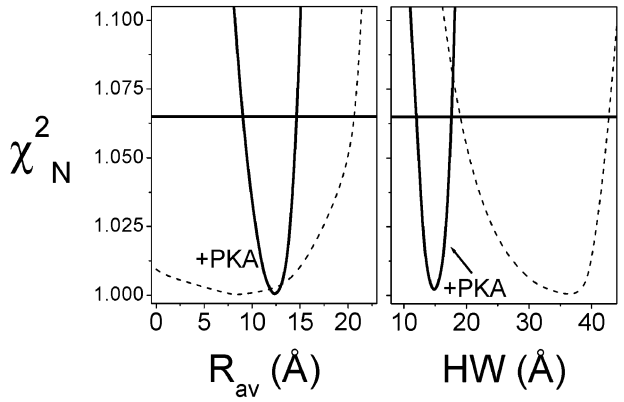

FIGURE 6: Depiction of error surfaces demonstrating phosphorylation-induced changes in conformational heterogeneity of the cytosolic domain of PLB. Experimental curves correspond to parameter values for average donor−acceptor separation (R_{av}) and associated half-width (HW) for a model involving a Gaussian distribution of the donor−acceptor distance. There are at least three independent data sets for PLB in the absence (dashed line) or presence (solid line) of PKA. Error surfaces were constructed by incrementally adjusting either R_{av} or HW and allowing all other parameters to vary in the least-squares analysis, which provides a conservative estimate of phosphorylation-induced changes in the recovered values (*56*). The horizontal line corresponds to the *F*-statistic for one standard deviation. Experimental conditions are as described in the legend to Figure 5.

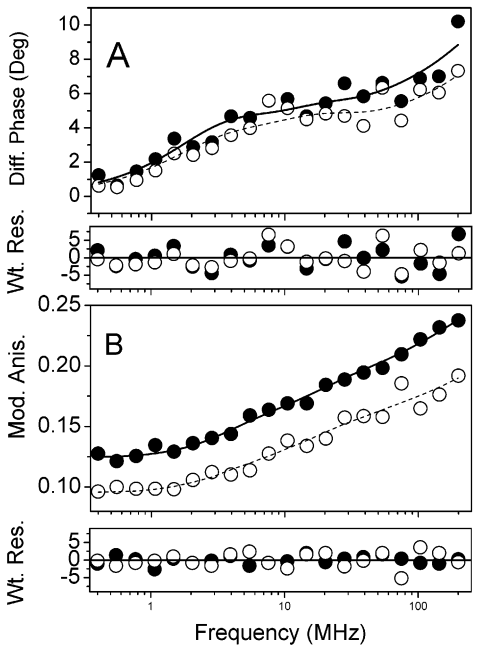

FIGURE 7: Fluorescence anisotropy decays for PMal−PLB before (●, —) or after (○, ---) phosphorylation by PKA. Measured differential phase angles and modulated anisotropies (●, ○) and associated nonlinear least-squares fits to the three-exponential model (—, ---) with weighted residuals (Wt. Res.) are shown below respective data sets. Experimental conditions are as described in the legend to Figure 5.

the presence of two well-defined conformations for the cytoplasmic domain of PLB that are modulated by the PKA-dependent phosphorylation of PLB (Figure 6). These results provide strong evidence that phosphorylation directly modulates the conformation of PLB and suggest a possible involvement of the flexible hinge region.

Dynamics of Transmembrane Domain. To further assess the structural properties of PLB, we have measured the rotational dynamics of PMal covalently bound to Cys[24] in PLB using frequency-domain fluorescence anisotropy methods. These measurements resolve both the segmental rotational motion associated with PMal and changes in the global motions of the transmembrane domain of PLB. The differential phase and modulated anisotropy were measured over 20 frequencies between 0.4 and 200 MHz (Figure 7). One observes that there is a progressive increase in both the differential phase and modulated anisotropy as the frequency increases and that there are substantial differences resulting from the phosphorylation of PLB that are most readily apparent in the frequency-independent reduction of the modulated anisotropy (Figure 7B). These results clearly demonstrate a phosphorylation-induced change in the frequency response of both the differential phase and modulated anisotropy.

However, as the frequency response is sensitive to both changes in the lifetime and rotational dynamics of the chromophore, a quantitative consideration of the frequency responses of the differential phase and modulated anisotropy requires that the data be fit using the method of nonlinear least squares to a sum of exponentials. A quantitative description of the frequency responses before and after the phosphorylation of PLB by PKA requires a model involving three rates (Table 3), which are related to the independent motion of the probe and dynamic fluctuations in the backbone fold of PLB that are a reflection of its conformational heterogeneity (*57*). From these results it is, furthermore, clear that PMal does not detect any significant change in the backbone fold of PLB following phosphorylation. Thus, the observed differences in the frequency-domain anisotropy data are a reflection of the large increase in the mean lifetime of PMal covalently bound to Cys[24] following phosphorylation of PLB by PKA. These results emphasize that observed changes in the conformational heterogeneity between the cytosolic and transmembrane domains of PLB measured using FRET reflect alterations in their structural coupling rather than a global structural change involving the transmembrane domain. Furthermore, the large amplitude motions of PMal, coupled with the fact that both PMal and nitroTyr[6] are solvent exposed, suggest that donor and

acceptor chromophores are motionally averaged (i.e., $\kappa^2 = {}^2/_3$) and that errors in the calculations of distances from the FRET measurements are no larger than 3 Å (*15*, *31*, *40*, *43*, *58*).

DISCUSSION

Summary of Results. We have used FRET to measure both the spatial separation and conformational heterogeneity between the site-specific chromophores PMal covalently bound to Cys^{24} at the top of the transmembrane domain and nitroTyr^{6} within the cytosolic domain of PLB in the absence of the Ca-ATPase (Figure 1). These probes, which do not compromise the regulatory function of PLB, provide accurate structural measurements of PLB within bilayer lipids and in the absence of complicating interactions with the Ca-ATPase. Thus, this study focuses on responses of PLB structure to its phosphorylation at Ser^{16}, permitting an understanding of this conformational switch underlying the regulation of muscle contraction. Phosphorylation of PLB by PKA results in a global conformational change that brings these chromophores within the cytosolic and transmembrane domains into closer proximity, where the apparent spatial separation decreases by 3 Å from 21.1 ± 0.9 Å to 18.2 ± 0.6 Å (Figure 5, Table 1). There is considerable conformational heterogeneity in the recovered distance distribution (HW > 18.9 Å; Figure 6, Table 1), consistent with the presence of the flexible hinge element suggested by solution NMR measurements (*16*). Conformational heterogeneity is significantly reduced upon phosphorylation of PLB by PKA, without corresponding changes in the rotational dynamics of the transmembrane domain (Table 3), indicating that the average structure remains relatively unchanged. Thus, the phosphorylation-induced restriction of the conformational heterogeneity of PLB involves the stabilization of cytosolic secondary structural elements. In conjunction with the high-resolution NMR structure, these results suggest that this angular stabilization of the cytosolic structure involves conformational restriction within the flexible hinge connecting the cytosolic and transmembrane domains corresponding to a coil-to-helix transition (Figure 8). Such a phosphorylation-responsive switching mechanism has the potential to induce conformational rearrangements that affect functional interactions with the Ca-ATPase by disrupting binding interactions between residues near the amino terminus of PLB and sites on the nucleotide binding domain of the Ca-ATPase, located approximately 50 Å above the membrane surface. Binding to this site on the nucleotide binding domain requires PLB to adopt an extended and disordered structure (*18*, *19*). Phosphorylation stabilizes the helical structure of PLB near the hinge element, reducing the possible length of the cytosolic domain of PLB. Thus, physical constraints imposed by the maximal extension of the PLB structure require the release of the inhibitory interaction with the nucleotide binding domain of the Ca-ATPase following phosphorylation, permitting relaxation of the Ca-ATPase structure and restoration of enzyme function.

Structural Interaction between PLB and the Ca-ATPase. Prior measurements have demonstrated that PLB binds to a sequence (i.e., $KDDKPVK^{403}$) within the nucleotide binding domain of the Ca-ATPase (*5*, *59*, *60*). Before its phosphorylation by PKA, PLB binding stabilizes the backbone fold of the Ca-ATPase, reducing the amplitude of catalytically

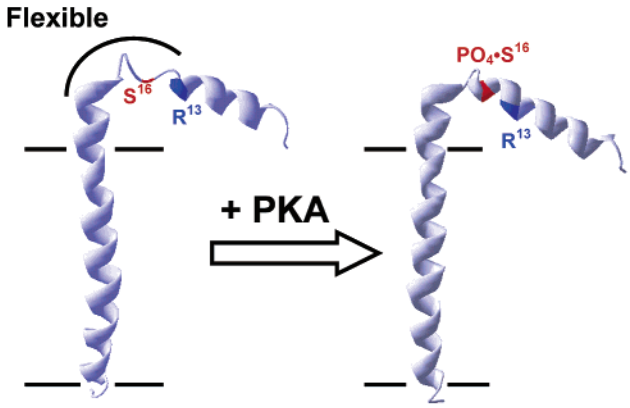

FIGURE 8: Model depicting phosphorylation-dependent stabilization of the backbone fold of PLB. Phosphorylation is depicted as stabilizing the helical structure in the cytosolic domain through the formation of a salt bridge between phosphoSer^{16} and Arg^{13} on the same face of the helix. A similar stabilization is possible following phosphorylation of Thr^{17} that may involve Arg^{14}. Depicted structures are models derived from coordinates 1FJK.pdb (*16*) using the program Swiss-Pdb viewer (*68*). Average orientations of cytosolic domains of PLB are arbitrary and do not represent the most probable conformation in the bilayer. Horizontal lines represent approximate positions of the bilayer surface.

important nucleotide domain motions associated with the transport mechanism of the Ca-ATPase (*9*−*13*, *57*, *61*). However, following phosphorylation, PLB remains associated with the Ca-ATPase, although the conformation near the lipid−water interface is altered to modulate the binding interface between PLB and the Ca-ATPase so as to release the inhibitory interaction (*15*, *31*, *62*). We report that phosphorylation of PLB at Ser^{16} restricts the conformational heterogeneity of the cytosolic domain through the stabilization of the backbone fold of PLB. Together, these results provide strong support for a model in which the phosphorylation-induced stabilization of the α-helical content of the cytosolic domain of PLB induces a conformational rearrangement between PLB and the Ca-ATPase that induces the formation of a new set of molecular interactions that no longer restrict catalytically important domain motions involving the nucleotide binding domain. Thus, prior to its phosphorylation, PLB associates with the Ca-ATPase in an extended structure that permits elements within the cytosolic and transmembrane domains of PLB to bind to spatially distant sites on the Ca-ATPase to inhibit function (*18*, *19*, *63*). Following phosphorylation and the stabilization of helix near the hinge element, PLB adopts a more compact structure that involves the formation of new interfacial contact interactions and the release of the inhibitory interaction associated with the nucleotide binding domain.

Structure of PLB. Critical to understanding the mechanism of inhibition is an elucidation of the structural changes associated with the phosphorylation of PLB that modulate Ca-ATPase function. Earlier FTIR measurements using synthesized PLB suggested a structure that was essentially completely helical with essentially no β-structure (*23*). In contrast, CD and FTIR measurements of wild-type or expressed PLB reconstituted into lipid bilayers suggest the presence of β-structure (*22*, *57*), which is consistent with the high-resolution NMR structure of PLB obtained in organic cosolvents (*16*). A distribution of structures were determined by Krebs and co-workers, whose spatial separa-

tion between the side chains at positions 24 and 6 (used in this study to attach chromophores for FRET measurements) varied between 19 and 25 Å (1FJK.pdb). Before phosphorylation, we observe that the apparent spatial separation between these sites in PLB reconstituted in lipid bilayers is less than 21 Å, which is consistent with the proposed structure (Table 1). However, the half-width of the distance distribution from FRET measurements is substantially larger than estimates from the NMR structure (HW = 36 Å; Figure 6). This apparent discrepancy may be related to either solution conditions (i.e., organic cosolvents vs reconstituted bilayers) or differences in the sensitivities of these methods to conformational disorder. Specifically, while NMR measurements favor the structure determination of ordered and highly populated states, fluorescence spectroscopy measurements resolve the full extent of conformational disorder (*43*). Irrespective of the underlying physical reason, these results suggest that the cytoplasmic domain adopts a larger range of orientations than depicted in the family of structures determined by Krebs and co-workers (*16*), suggesting greater conformational disorder within the hinge region of PLB than the average structure determined by these NMR measurements (Figure 1). Phosphorylation induces a significant reduction in the conformational heterogeneity of the cytosolic domain (HW = 15 Å; Figure 6). These results suggest a structural reorganization involving a reduction in the flexibility of the linker region interconnecting the cytosolic and transmembrane domains of PLB. The proximal arginine (i.e., Arg^{13}) lies on the same face of the helix proximal to Ser^{16} and can form electrostatic interactions with the phosphoryl group of $phosphoSer^{16}$ (Figure 8). The formation of this salt bridge would, furthermore, be expected to decrease the binding interaction between PLB and the inhibitory site on the Ca-ATPase, since prior to phosphorylation Arg^{13} in PLB is suggested to form a stabilizing hydrogen-bonding interaction with either Glu^{432} or Glu^{429} of the Ca-ATPase (*18*). We therefore suggest that the phosphorylation of Ser^{16} by PKA restricts the conformational heterogeneity of the cytosolic domain relative to the transmembrane sequence by the stabilization of the backbone fold of the linker region connecting the transmembrane and cytosolic domains of PLB. This coil-to-helix transition would, furthermore, reduce the maximal length of PLB. These results are in contrast to earlier measurements using peptides identical to the cytosolic domain of PLB, which suggested that phosphorylation disrupts the backbone fold between $Ala^{11}$and Ser^{16} (*21*, *64*, *65*). However, under the solution conditions used (i.e., pH 3.0 or 4.2) these peptides adopt largely unconstrained structures in aqueous solution; secondary structural assignments required the use of helix-promoting cosolvents. Under these conditions the negative charge density of the phosphoryl moiety may disrupt cosolvent−protein interactions important to maintaining structure. Thus, the present study provides the first indication that phosphorylation of PLB by PKA stabilizes the backbone fold of PLB. Given that PLB, by necessity, adopts an extended structure to form the favorable interaction between its cytosolic domain and the $KDDKPVK^{403}$ binding sequence within the Ca-ATPase (*18*, *19*), these results suggest that phosphorylation induces a coil-to-helix transition that effectively shortens the maximal extension of the cytosolic domain of PLB. We suggest that this steric restraint functions as a conformational switch to release the inhibitory interaction between PLB and the nucleotide binding domain of the Ca-ATPase.

Conclusions and Future Directions. We have demonstrated that phosphorylation of Ser^{16} in PLB by PKA induces a structural rearrangement between the cytosolic and transmembrane domains of PLB. Before its phosphorylation PLB assumes a wide range of conformations, which may facilitate its molecular interaction with the Ca-ATPase so as to inhibit function. Following phosphorylation of PLB, the backbone fold is stabilized, resulting in a reduction in the observed conformational heterogeneity. These results suggest that phosphorylation functions as a switching mechanism that modulates the binding interaction between PLB and the Ca-ATPase to modulate function. Future results should seek to clarify how phosphorylation modulates the precise binding interactions between PLB and the Ca-ATPase to identify the molecular details associated with conformational switching.

ACKNOWLEDGMENT

We thank Dr. Yijia Xiong for helpful discussions.

REFERENCES

1. Tada, M., Kirchberger, M. A., and Katz, A. M. (1975) *J. Biol. Chem. 250*, 2640−2647.
2. Lindemann, J. P., Jones, L. R., Hathaway, D. R., Henry, B. G., and Watanabe, A. M. (1983) *J. Biol. Chem. 258*, 464−471.
3. Kranias, E. G. (1985) *J. Biol. Chem. 260*, 11006−11010.
4. Inui, M., Chamberlain, B. H., Saito, A., and Fleischer, S. (1986) *J. Biol. Chem. 261*, 1794−1800.
5. James, P., Inui, M., Tada, M., Chiesi, M., and Carafoli, E. (1989) *Nature 342*, 90−92.
6. Wegener, A. D., Simmerman, H. K. B., Lindemann, J. P., and Jones, L. R. (1989) *J. Biol. Chem. 264*, 11468−11474.
7. Sasaki, T., Inui, M., Kimura, Y., Kuzuya, T., and Tada, M. (1992) *Biol. Chem. 267*, 1674−1679.
8. Simmerman, H. K. B., and Jones, L. R. (1998) *Physiol. Rev. 78*, 921−947.
9. Negash, S., Chen, L. T., Bigelow, D. J., and Squier, T. C. (1996) *Biochemistry 35*, 11247−11258.
10. Huang, S., Negash, S., and Squier, T. C. (1998) *Biochemistry 37*, 6949−6957.
11. Negash, S., Huang, S., and Squier, T. C. (1999) *Biochemistry 38*, 8150−8158.
12. Toyoshima, C., Nakasako, M., Nomura, H., and Ogawa, H. (2000) *Nature 405*, 647−655.
13. Toyoshima, C., and Nomura, H. (2002) *Nature 418*, 605−611.
14. Stokes, D. L., and Green, N. M. (2003) *Annu. Rev. Biophys. Biomol. Struct. 32*, 445−468.
15. Chen, B., and Bigelow, D. J. (2002) *Biochemistry 41*, 13965−13972.
16. Lamberth, S., Schmid, H., Muenchbach, M., Vorherr, T., Krebs, J., Carafoli, E., and Griesinger, C. (2000) *Helv. Chim. Acta 83*, 2141−2152.
17. Young, H. S., Jones, L. R., and Stokes, D. L. (2001) *Biophys. J. 81*, 884−894.
18. Hutter, M. C., Krebs, J., Meiler, J., Griesinger, C., Carafoli, E., and Helms, V. (2002) *ChemBioChem. 3*, 1200−1208.
19. Toyoshima, C., Asahi, M., Sugita, Y., Khanna, R. Tsuda, T., and MacLennan, D. H. (2003) *Proc. Natl. Acad. Sci. U.S.A. 100*, 467−472.
20. Pollesello, P., Annila, A., and Ovaska, M. (1999) *Biophys. J. 76*, 1784−1795.
21. Pollesello, P., and Annila, A. (2002) *Biophys. J. 83*, 484−490.
22. Tatulian, S. A., Jones, L. R., Reddy, L. G., Stokes, D. L., and Tamm, L. K. (1995) *Biochemistry 34*, 4448−4456.
23. Arkin, I. T., Rothman, M., Ludlam, C. F., Aimoto, S., Engelman, D. M., Rothschild, K. J., and Smith, S. O. (1995) *J. Mol. Biol. 248*, 824−835.
24. Smith, S. O., Kawakami, T., Liu, W., Ziliox, M., and Aimoto, S. (2001) *J. Mol. Biol. 313*, 1139−1148.
25. Mascioni, A., Karim, C., Zamoon, J., Thomas, D. D., and Veglia, G. (2002) *J. Am. Chem. Soc. 124*, 9392−9393.

26. Kirby, T. L., Karim, C. B., and Thomas, D. D. (2003) *Biophys. J. 84*, 264a.
27. Chen, P. S., Toribara, T. Y., and Warner, H. (1965) *Anal. Chem. 28*, 1756−1758.
28. Fernandez, J. L., Rosemblatt, M., and Hidalgo, C. (1980) *Biochim. Biophys. Acta 599*, 552−568.
29. Yao, Q., Chen, L. T., and Bigelow, D. J. (1998) *Protein Expression Purif. 13*, 191−197.
30. Yao, Q., Bevan, J. L., Weaver, R. F., and Bigelow, D. J. (1996) *Protein Expression Purif. 8*, 463−468.
31. Negash, S., Yao, Q., Sun, H., Li, J., Bigelow, D. J., and Squier, T. C. (2000) *Biochem. J. 351*, 195−205.
32. Schaffner, W., and Weissmann, C. (1973) *Anal. Biochem. 56*, 502−514.
33. Lanzetta, P. A., Alvarez, L. J., Reinach, P. S., and Candia, D. A. (1979) *Anal. Biochem. 100*, 95−97.
34. Fabiato, A. (1988) *Methods Enzymol. 157*, 378−417.
35. Richman, P. G., and Klee, C. B. (1978) *Biochemistry 17*, 928−935.
36. Yao, Y., Schoneich, C., and Squier, T. C. (1994) *Biochemistry 33*, 7797−7810.
37. Haugland, R. P. (2003) *Handbook of Fluorescent Probes and Research Chemicals*, 9th ed., Molecular Probes, Eugene, OR.
38. Riordan, J. F., and Vallee, B. L. (1972) *Methods Enzymol. 25*, 515−521.
39. Hunter, G. W., and Squier, T. C. (1998) *Biochim. Biophys. Acta 1415*, 63−76.
40. Haas, E., Katchalski-Katzir, E., and Steinberg, I. (1978) *Biochemistry 17*, 5064−5070.
41. Weber, G. (1981) *J. Phys. Chem. 85*, 949−953.
42. Beechem, J. M., and Haas, E. (1989) *Biophys. J. 55*, 1225−1236.
43. Cheung, H. C. (1991) in *Topics in Fluorescence Spectroscopy* (Lakowicz, J. R., Ed.) Vol. 2, pp 128−176, Plenum Press, New York.
44. Sun, H., Yin, D., and Squier, T. C. (1999) *Biochemistry 38*, 12266−12279.
45. Lakowicz, J. R., Gryczynski, I., Wiczk, W., Kusba, J., and Johnson, M. L. (1991) *Anal. Biochem. 195*, 243−254.
46. Bevington, P. R. (1969) in *Data Reduction and Error Analysis for the Physical Sciences*, McGraw-Hill, New York.
47. Lakowicz, J. R., and Gryczynski, I.. (1991) in *Topics in Fluorescence Spectroscopy* (Lakowicz, J. R., Ed.) Vol. 1, pp 293−335, Plenum Press, New York.
48. Fujii, J., Maruyama, K., Tada, M., and MacLennan, D. H. (1989) *J. Biol. Chem. 264*, 12950−12955.
49. Kimura, Y., Kurzydlowski, K., Tada, M., and MacLennan, D. H. (1997) *J. Biol. Chem. 272*, 15061−15064.
50. Karim, C. B., Paterlin, M. G., Reddy, L. G., Hunter, G. W., Barany, G., and Thomas, D. D. (2001) *J. Biol. Chem. 276*, 38814−38819.
51. Li, M., Reddy, L. G., Bennett, R., Silva, N., Jones, L. R., and Thomas, D. D. (1999) *Biophys. J. 76*, 2587−2599.
52. Bers, D. M. (2001) *Excitation-contraction coupling and cardiac contractile force*, 2nd ed., Chapter 7, pp 164−169, Kluwer Academic Publishers, Boston.
53. Ferrington, D. A., Yao, Q., Squier, T. C., and Bigelow, D. J. (2002) *Biochemistry 41*, 13289−13296.
54. Yao, Q., Chen, L. T. L., Brungardt, K., Squier, T. C., and Bigelow, D. J. (2001) *Biochemistry 40*, 6406−6413.
55. Sun, H., Yin, D., Coffeen, L. A., Shea, M. A., and Squier, T. C. (2001) *Biochemistry 40*, 9605−9617.
56. Beechem, J. M., Gratton, E., Ameloot, M., Knutson, J. R., and Brand, L. (1991) *Topics in Fluorescence Spectroscopy* (Lakowicz, J. R., Ed.) Vol. 2, pp 241−306, Plenum Press, New York.
57. Tatulian, S. A., Chen, B., Li, J., Negash, S., Middaugh, C. R., Bigelow, D. J., and Squier, T. C. (2002) *Biochemistry 41*, 741−751.
58. Wu, P., and Brand, L. (1992) *Biochemistry 31*, 7939−7947.
59. Toyofuku, T., Kurzydlowski, K., Tada, M., and MacLennan, D. H. (1994) *J. Biol. Chem. 269*, 22929−22932.
60. MacLennan, D. H., Kumura, Y., and Toyofuku, T. (1998) *Ann. N.Y. Acad. Sci. 853*, 31−42.
61. Inesi, G., Zhang, Z., and Lewis, D. (2002) *Biophys. J. 83*, 2327−2332.
62. Asahi, M., McKenna, E., Kurzydlowski, K., Tada, M., and MacLennan, D. H. (2000) *J. Biol. Chem. 275*, 15034−15038.
63. MacLennan, D. H., and Kranias, E. G. (2003) *Nat. Rev. Mol. Cell. Biol. 4*, 566−577.
64. Terzi, E., Poteur, L., and Trifilieff, E. (1992) *FEBS Lett. 309*, 413−416.
65. Mortishire-Smith, R. J., Broughton, H., Garsky, V. M., Mayer, E. J., and Johnson, R. G. (1998) *Ann. N.Y. Acad. Sci. 853*, 63−78.
66. Fairclough, R. H., and Cantor, C. R. (1978) *Methods Enzymol. 48*, 347−379.
67. Stryer, L. (1978) *Annu. Rev. Biochem. 47*, 819−846.
68. Guex, N., and Peitsch, M. C. (1997) *Electrophoresis 18*, 2714−2723.

BI034708C